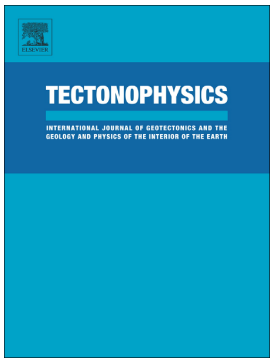

Sandstone provenance analysis in Longyan supports the existence of a Late Paleozoic continental arc in South China

Chao Li, Xiumian Hu, Jiangang Wang, Pieter Vermeesch, Eduardo Garzanti

PII: S0040-1951(20)30083-4

DOI: https://doi.org/10.1016/j.tecto.2020.228400

Reference: TECTO 228400

To appear in: *Tectonophysics*

Received date: 15 October 2019

Revised date: 16 February 2020

Accepted date: 10 March 2020

Please cite this article as: C. Li, X. Hu, J. Wang, et al., Sandstone provenance analysis in Longyan supports the existence of a Late Paleozoic continental arc in South China, *Tectonophysics*(2018), https://doi.org/10.1016/j.tecto.2020.228400

Sandstone provenance analysis in Longyan supports the existence of a Late Paleozoic continental arc in South China

Chao Li[1, 2], Xiumian Hu[1], Jiangang Wang[3], Pieter Vermeesch[4], Eduardo Garzanti[5]

1 State Key Laboratory of Mineral Deposit Research, School of Earth Sciences and Engineering, Nanjing University, Nanjing 210023, China

2 State Key Laboratory of Oil and Gas Reservoir Geology and Exploitation (Chengdu University of Technology), Institute of Sedimentary Geology, Chengdu 610059, China

3 State Key Laboratory of Lithospheric Evolution, Institute of Geology and Geophysics, Chinese Academy of Sciences, Beijing 100029, China

4 London Geochronology Centre, University College London, London WC1E 6BT, United Kingdom

5 Department of Earth and Environmental Sciences, Università di Milano-Bicocca, Milano 20126, Italy

*Corresponding author: Dr. Xiumian Hu

E-mail: huxm@nju.edu.cn; Tel: 0086 25 89683002; 139 5185 8070

Abstract

Because of the limited magmatic and metamorphic record, the Late Paleozoic tectonic setting in South China remains controversial. This paper presents sedimentologic data and provenance analysis of Upper Paleozoic sandstones in Longyan, which are rich in quartz (73-90%) and poor in lithic fragments (2-12%) and feldspar (3-25%). Devonian sandstones contain mostly metamorphic lithic fragments (e.g., quartzite), whereas Carboniferous-Permian sandstones contain mostly felsic volcanic and subvolcanic lithic fragments indicating provenance from felsic volcanic rocks.

Detrital zircon U-Pb age spectra of Devonian-Carboniferous sandstones display modes at ~440 Ma and 420-380 Ma, with subordinate Mesoproterozoic age components, pointing at the Nanling terrane and the western-middle part of the Wuyi terrane as most likely ultimate sediment sources. Permian sandstones inherited the age components mentioned above, but also include peaks at ~290 Ma and ~1850 Ma. The ~290 Ma component corresponds to the age of Late Paleozoic magmatism in southeastern China and southwest Japan. Numerous detrital zircons aged at 350-250 Ma also occur in Permo-Triassic strata exposed across South China and southwest Japan. Based on regional data and on the ages and Hf isotope signatures of detrital zircon, we infer that a Late Paleozoic continental arc existed in the coastal area of southeastern China and contributed detritus to the adjacent sedimentary basins. The Permo-Triassic igneous rocks locally exposed in the area may represent the remnant of that continental arc. Arc growth may have been responsible for the westward retreat of a broad Upper Paleozoic carbonate platform.

Key words: South China; Late Paleozoic; sedimentary provenance; tectonic setting; continental arc; carbonate platform

1. Introduction

During the Mesozoic, South China experienced widespread magmatism. Although different scenarios have been proposed to explain this Mesozoic igneous activity (Zhou and Li, 2000; Li and Li, 2007), the consensus is that there was an active margin generated by the subduction of the paleo-Pacific plate beneath South China at the time. However, it is still unclear how this active margin was generated and which was the tectonic environment of the area during the Late Paleozoic. The answers to these questions are crucial for palaeogeographic reconstructions because South China lay at the eastern edge of Pangea supercontinent (Scotese, 2016), and the transition from passive-margin to active-margin settings thus marked the initiation of a subduction

zone encircling the Paleo-Pacific (or Panthalassa) ocean plate (Shen et al., 2018).

Some researchers have hypothesized that a subduction-related continental arc existed along the eastern margin of South China during the Early Permian. Sedimentological and provenance data from Permian sandstones in South China and southwest Japan suggest that these were deposited in a retroarc basin (Li et al., 2012; Hu et al., 2015; Li et al., 2017; Zhang et al., 2019), an interpretation corroborated by geochemical data on potential source rocks exposed in Hainan Island, South China (Li et al., 2006).

Other researchers proposed that an island arc existed offshore of South China during the Late Carboniferous to Early Permian. According to that model, a back-arc basin was present at those times along the margin of present-day South China, as suggested by geochemical data from Carboniferous to Permian igneous rocks in South China and Japan that point at an extensional or transtensional setting (Wang et al., 2005; Hara et al., 2018; Shen et al., 2018). The island arc would have been subsequently accreted onto South China during the Middle Permian

The present study investigates the provenance of Upper Devonian to Upper Permian sedimentary rocks in the Longyan area of southeastern China (Fig. 1) by combining original data with a comprehensive review of previously published information. This integrated dataset indicates expansion of the source areas in the Middle Permian and retreat of a wide carbonate platform from the Early Permian to the Late Permian. We provide evidence that the growth of a Late Paleozoic continental arc in South China represented a main controlling factor of both processes.

2. Regional geology

2.1. Tectonic background

The South China Block consists of the Yangtze block to the north and the Cathaysian block to the south (Fig. 1). These two terranes were assembled along the

northeast-trending Jiangshan-Shaoxing fault zone in the Neoproterozoic, although different opinions exist concerning the exact timing (Wang et al., 2007; Li et al., 2009). The boundary between different regions and the early history of the Cathaysian block remain unclear (Zhao and Cawood., 2012; Li et al., 2014).

The Cathaysia block is subdivided into three parts according to Shu (2006) and in two parts separated by the Zhenghe-Dapu Fault according to Xu (2007) (Fig. 1). The similarity of basement rocks on both sides of the Zhenghe-Dapu Fault, however, indicates that Zhenghe-Dapu Fault cannot represent a first-order tectonic boundary (Yu et al., 2010). The southeastern Cathaysia block includes a Precambrian basement and is dominated by Upper Mesozoic igneous rocks (Xu et al., 2007). The northwestern Cathaysian block, instead, is an Early Paleozoic fold-thrust belt including pre-Cenozoic igneous rocks and sedimentary rocks overlying Precambrian basement (Li et al., 1997; Wan et al., 2007; Yu et al., 2009).

The northwestern part of the Cathaysian block can be further subdivided into the Nanling-Yunkai and Wuyi terranes (Yu et al., 2010) (Fig. 1). The boundary between these two terranes possibly follows a line connecting the modern cities of Xunwu and Meixian (Yu et al., 2010). U-Pb zircon age data from metasedimentary and igneous rocks showed that the Nanling-Yunkai terrane has undergone six stages of crustal growth, at ~3.6 Ga, ~3.3 Ga, 2.5-2.6 Ga, ~1.6 Ga, ~1.0 Ga, and 0.8-0.7 Ga, whereas the Wuyi terrane experienced five main phases of igneous activity, at ~3.6 Ga, ~2.8 Ga, 2.6-2.4 Ga, ~1.85 Ga, and 0.8-0.7 Ga (Yu et al., 2010). The oldest rocks of the Cathaysian block are the Upper Paleoproterozoic igneous and metamorphic rocks exposed in southwest Zhejiang and northwest Fujian (Li et al., 1997; Wan et al., 2007; Yu et al., 2009; Xia et al., 2012;). The studied Longyan area is located in the western part of the Wuyi terrane, near the intersection between the Zhenghe-Dapu Fault and the Xunwu – Meixian line (Fig. 1).

South China is considered to have been much wider before the Cenozoic when it

included parts of the present-day Korean Peninsula and southwest Japan (Isozaki et al., 2017). An orogen named the Kurosegawa Belt, located at the southeastern edge of South China since at least Triassic time and containing Ordovician to Permian igneous and metamorphic rocks, and Permian to Jurassic shallow marine accretionary complexes (Hara et al., 2018), has drifted to its present location after the Cretaceous (Uno et al., 2011).

2.2. Stratigraphic framework

In the Longyan area, folded anchimetamorphic Cambrian strata are overlain in angular unconformity associated with the Early Paleozoic Kwangsian orogeny by Upper Paleozoic sedimentary cover rocks. Intervening Ordovician to lower Devonian strata are lacking. The lithology, sedimentary structures and depositional environment of the exposed stratigraphic units are described below according to previous paleogeographic studies and our own field observations (Fig.2).

The Cambrian Lintian Formation ($\in_{1\text{-}3}l$) is dominated by fine-grained feldspatho-quartzose metasandstone, and phyllite or slate originally deposited in a low-energy shelfal or deep-water offshore environment (Fujian Institute of Geological Survey, 2015).

The 877 m-thick Upper Devonian Tianwadong Formation (D_3t) consists of two members. The lower member is dominated by poorly sorted clast-supported quartzose conglomerate, whereas the upper member is dominated by siltstone and mudrocks with pebbly quartzose sandstone. Pebbles ranging 1-5 cm in diameter are sub-rounded and mostly consist of vein quartz, chert, and locally metasandstone. Clast imbrication with inclination angles between 10° and 20° indicates upper flow regime (Fig. S1; Fig. S2). Several fining-upward cycles with basal erosive surface and oblique lamination are observed. Sediments of the Tianwadong Formation were most likely deposited in a braided-river environment (Liu et al., 1994; Fujian Institute of Geological Survey

(2015)

The 766 m-thick Upper Devonian Taozikeng Formation (D_3tz) lies in conformable contact onto the Tianwadong Formation. Two members can be distinguished. The lower member mainly consists of pebbly quartzose sandstone intercalated with thin-quartzose sandstone and mudrocks. The upper member mainly consists of mudrocks, with moderately sorted quartzose conglomerate and pebbly sandstone. Small rounded pebbles 0.2-1 cm in diameter mainly consist of vein quartz or chert (Fig. S1; Fig. S2). Fining-upward cycles with basal erosive surfaces, parallel and oblique lamination indicate a fluvial (Liu et al., 1994; Fujian Institute of Geological Survey, 2015) and probably braided-river depositional environment.

The 182 m-thick Lower Carboniferous Lindi Formation (C_1l) unconformably overlies the Taozikeng Formation and is dominated by moderately sorted quartzose pebbly sandstone and conglomerate with minor mudrocks. Small pebbles 0.3 cm in average diameter are subangular and mainly consist of quartzose sandstone and quartzite (Fig. S1; Fig. S2). Fining upward cycles with basal erosive surfaces and clast imbrication are locally observed. A fluvial (Liu et al., 1994; Fujian Institute of Geological Survey, 2015) and probably braided-river depositional environment is indicated.

The 168 m-thick Upper Carboniferous Jingshe Formation (C_2j) unconformably overlies the Lindi Formation and mainly consists of bioclastic limestone including corals and brachiopods interbedded with mudstone, indicating a shallow-marine environment (Fujian Institute of Geological Survey, 2015).

The 88 m-thick Lower Permian Chuanshan Formation (P_1c), lying in conformable contact on the Jingshe Formation, mainly consists of thick-bedded bioclastic limestone. The conformably overlying 157 m-thick Permian Qixia Formation (P_2q) is dominated by bioclastic (fusulinids, corals, and brachiopod) micritic limestone with chert layers or nodules (Fig. S2) with intercalated thin layers of siliciclastic rocks. Lithology and fossils indicate that the Chuanshan Formation (P_1c) and the Qixia

Formation (P_2q) were deposited in a stable, warm, shallow-water carbonate platform widely distributed in South China (Liu et al., 1994; Fujian Institute of Geological Survey, 2015).

The 58 m-thick Middle Permian Wenbishan Formation (P_2w) mainly consists of shale, siltstone, and fine sandstone containing abundant ammonites, brachiopods, bivalves and locally trilobites and crinoids, documenting the reappearance of terrigenous detritus (Fig. S2) in a shallow-marine setting (Fujian Institute of Geological Survey, 2015).

The 585 m-thick Middle Permian Tongziyan Formation (P_2t) conformably overlies the Wenbishan Formation and mostly consists of fine sandstone with intercalated mudrocks (Fig. S1; Fig. S2). Clinoforms and mudstone pebbles suggest a delta-front depositional environment passing upward to a delta-plain swamp, as indicated by thin coal beds and abundant plant fragments in the upper part of the unit (Fujian Institute of Geological Survey, 2015).

The 495 m-thick Upper Permian Cuipingshan Formation (P_3cp) lies in unconformable contact onto the Tongziyan Formation and mainly consists of quartzose sandstone, mudrocks and locally thin lenses of coal (Fig.S2). Pebbly conglomerate to coarse sandstone at the base contain plant fossils. The 93 m-thick Upper Permian Luokeng Formation (P_3l) mainly consists of marl interbedded with fine feldspatho-quartzose sandstone (Fig. S2). These two Upper Permian units were also deposited in a delta front to delta plain environment (Fujian Institute of Geological Survey, 2015).

3. Sampling and methods

One meta-sandstone from Cambrian strata and eighteen samples from Upper Devonian to Upper Permian sandstones were collected (see Supplementary Table S1 for detailed information).

3.1. Sandstone petrography

The petrographic analysis was carried out by counting at least 400 framework grains on each thin section following the Gazzi-Dickinson point-counting method (i.e., crystals or grains larger than 62.5 μm in diameter within rock fragments are counted as single minerals; Ingersoll et al., 1984).

Sandstones were classified using composite adjectives that reflect the relative abundance of the three main framework components quartz, feldspar, and lithic fragments, provided they exceed 10% QFL. According to standard use, the less abundant component goes first, the more abundant last (e.g., in a litho-feldspatho-quartzose sand Q > F > L > 10% QFL; classification scheme after Garzanti 2019).

3.2. U-Pb Zircon Dating and Hf isotopes

Zircon grains were handpicked randomly from heavy-mineral concentrates. The selected zircons were then mounted in epoxy resin and polished to expose the crystal interior. U-Pb dating was conducted by LA-ICP-MS at the State Key Laboratory for Mineral Deposits Research, Nanjing University, China, following the method proposed by Jackson et al. (2004) with a beam diameter of 35 μm. GLITTER 4.4 was used for calculating results and relevant isotopic rates (Jackson et al., 2004). Kernel Density Estimation plots are used to visualize the results (generated by the Java-based *DensityPlotter* program of Vermeesch, 2012). We applied a 15% discordance filter to the data and only retained ages whose analytical uncertainty was lower than 45Ma (1 σ). Each sample contained at least 60 concordant ages, ensuring with 95% confidence that no age component greater than 8.5% of the total was missed. We considered $^{206}Pb/^{238}U$ ages for grains <1000 Ma and $^{207}Pb/^{206}Pb$ ages for grains >1000 Ma. (Vermeesch, 2004).

Zircon Hf isotope analysis was performed on a Neptune Multi-Collector ICP–MS equipped with the Geolas 193 laser-ablation system at the State Key Laboratory of Lithosphere Evolution, Institute of Geology and Geophysics, Chinese Academy of Sciences. Details on instrument conditions and data acquisition are illustrated in Wu et al. (2006). *In situ* Hf isotopic analyses were conducted in the same zone of zircon crystals previously analyzed for U-Pb dating, with a beam size of 60 μm. *In situ* Hf isotopic data are provided in Supplementary Table S3.

4. Results

4.1. Sandstone petrography

All Paleozoic sandstones are rich in quartz (73-90%) and poor in lithic fragments (3-12%) (Fig. 3a). Feldspar content varies widely from 3% to 25%, and increases slightly from Devonian to Carboniferous and Permian sandstones (Table 1). Two sandstone groups can be distinguished based on lithic content. Devonian sandstones (Tianwadong and Taozikeng Fms.) mostly contain quartzite and other metamorphic lithics (Lm 52 - 86, Lv 14-48, Ls ≤ 9%; Fig. 3b). Carboniferous and Permian sandstones, instead, mainly contain felsic volcanic rock fragments with quartz phenocrysts set in a felsitic groundmass (Lv 62-83).

4.2. Detrital zircon U-Pb dating

In total, 555 zircon grains from 7 samples yielded 499 concordant ages. Most zircons are euhedral to subhedral, with oscillatory zoning highlighted by cathodo-luminescence observations (Supplementary Figure S3). Among zircon grains, only 11 have Th/U <0.1 whereas 469 have Th/U >0.4 (Supplementary Table S2). These features indicate a mostly magmatic origin (Wu and Zheng, 2004).

According to their zircon age spectra, three groups of sandstone samples can be

identified (Fig. 4):

Group 1. The Cambrian sandstone sample 08TZK01 (Lintian Fm., $Є_{1-3}l$) yielded 71 concordant ages out of 84 zircon grains, ranging from 581 to 3576 Ma. Four modes occur at ~940 Ma (21%), 1400-1200 Ma (10%), ~1750 Ma (13%), and ~2500 Ma (17%),

Group 2. Upper Devonian to Lower Carboniferous sandstone samples 08TZK05 (Tianwadong Fm., D_3t) and 10TZK24 and 10LB06 (Lindi Fm., C_1l) share similar age spectra and yielded 217 concordant ages out of 229 zircon grains. The dominant age cluster occurs between 380 and 480 Ma (56%) with three peaks at ~390 Ma (26%, present only in the Lindi Formation, C_1l), ~420 Ma (15%), and ~440 Ma (15%). Age components ranging from 680 to 1250 Ma (27%) are subordinate.

Group 3. Middle-Upper Permian sandstones samples 08MTK04 (Tongziyan Fm., P_2t), 08MTK05 (Cuipingshan Fm., P_3cp), and 08MTK07 (Luokeng Fm., P_3l) yielded 211 concordant ages out of 242 detrital zircons. Similarly as in Group 2, age peaks occur at ~370 Ma (10%), ~420 Ma (9%), and ~440 Ma (8%), with subordinate age components clustering between 800 and 1270 Ma (24%). However, an additional younger peak occurs at ~290 Ma (10 %) together with more Paleoproterozoic ages ranging from 1600 to 1900 Ma (14%) and with peak at ~1750 Ma (Tongziyan Fm.) or ~1850 Ma (Cuipingshan and Luokeng Fms.).

4.3. *In situ* Hf isotopes

In Upper Devonian to Lower Carboniferous sandstones, zircon grains younger than 500 Ma are characterized by εHf (t) values ranging between -12 and 11 (average -4), whereas εHf (t) values in zircons older than 500 Ma range between -28 and +8 (average -7).

In Middle-Upper Permian sandstones, zircon grains younger than 500 Ma are

characterized by εHf (t) values ranging widely between -24 and +13 (average -6). As shown in Fig. 5b, the εHf (t) values are lower in grains aged between 500 and 390 Ma but higher again in grains younger than 390 Ma. Zircon grains older than 500 Ma are characterized by εHf (t) values ranging between -32 and +12 (average -3).

5. Discussion

5.1. Provenance interpretation

The Upper Devonian-Lower Carboniferous and Middle-Upper Permian sandstones of the Longyan area significantly differ in their petrographic and detrital-zircon signatures.

5.1.1 Upper Devonian-Lower Carboniferous sandstones

Dominantly coarse-grained sandstones and conglomerates rich in quartz and with roughly equi-abundant feldspar and lithic fragments (Fig. 3a; Fig. S2) may suggest a continental-block source, although an orogenic source cannot be ruled out. Zircon U-Pb age spectra are similar in the Lindi and Tianwadong formations, pointing at source rocks generated around 420 Ma and 440 Ma during the Kwangsian orogenesis and widespread both in the Wuyi and Nanling-Yunkai terranes of the Cathaysia block (Fig. 1). The older zircons may have been derived, directly or indirectly through recycling of older sandstones (e.g., Cambrian sandstones containing Neoproterozoic and Mesoproterozoic zircons; Fig. 4), from diverse sources. Grains aged 932-976 Ma may have been ultimately derived from the eastern part of the Nanling-Yunkai terrane, where a rhyolite dated as 972±8 Ma is exposed ~150 km southwest of Longyan (Fig. 1; Shu et al., 2008b). Grains aged 758-785 Ma may have been derived from the western and middle parts of the Wuyi terrane (Wang et al., 2010), where metavolcanic rock dated as 788±27 Ma (Li et al., 2010) and granitoid gneisses dated as 728-751 Ma (Wan et al., 2007) are exposed in the Sanming area, ~150 km northeast of Longyan.

Upper Devonian and Lower Carboniferous sandstones were thus most likely derived locally, not farther than the Nanling terrane and western-middle part of the Wuyi terrane (Fig. 8a). Because of the limited knowledge of Devonian-Carboniferous palaeogeography and the possibility of zircon recycling, however, other potential sources cannot be ruled out.

Peculiar to the Lindi Formation is the occurrence of young zircons dated as 380-400 Ma (Fig. 4). Subhedral or euhedral habit, oscillatory zoning, and Th/U ratio between 0.55 to 1.48 indicate a magmatic origin for these zircons, and their narrow spread of εHf (t) values from -3.38 to -8.61 suggests a specific igneous source rock. Similarly aged zircons occur in Permian sandstones in the Yongding (360-400 Ma; Li et al., 2012) and Shizhong areas (382-394 Ma; Hu et al., 2015), located 30 km to the SW and SE of the studied Longyan area, respectively. We conclude that felsic igneous rocks must have intruded the source area shortly before the deposition of the Lindi Formation, including the Xiqin and Xixi monzogranites (zircon U-Pb ages 399.1±1.6 Ma and 395 Ma, respectively) located 190 km to the NE and 50 km to the SW of the Longyan area (Fujian Institute of Geological Survey, 2015).

5.1.2 Middle-Upper Permian sandstones

During the Permian, mainly feldspatho-quartzose sandstones with mostly felsic volcanic or subvolcanic lithics were deposited in deltaic to shallow-marine environments (Fig. S2). Age spectra of zircon grains include the same components of older sandstones with additional younger (~290 Ma in the Tongziyan, Cuipingshan, and Luoping Fms.) and older ages (~1850 Ma; Cuipingshan and Luoping Fms.).

The Paleoproterozoic basement of the Cathaysia block, exposed in the eastern and central parts of the Wuyi terrane (Li, 1997; Yao et al., 2014) > 400 km to the NE of the Longyan area, mainly consists of granites or amphibole-facies metamorphic rocks dated as ~1850 Ma (Xia et al., 2012). These rocks may well represent the source of

Permo-Triassic sandstones exposed near Longyan (Hu et al., 2015), consistently with both their northeastward paleocurrents (Li, 1997) and the inferred Paleozoic palaeogeography of South China (Ma et al., 2009). The occurrence of ~1850 Ma detrital zircons in Upper Permian sandstones may thus suggest an eastward expansion of the source area. However, these old zircons may also be recycled from the Paleoproterozoic Tianjingping Fm., Neoproterozoic Dikou Fm., and/or Neoproterozoic-lower Paleozoic Mayuan Group exposed NW of Fujian, ~150 km north of Longyan, which all contain ~1850 Ma-aged zircons (e.g., Li, 1997; Wan et al., 2007; Li et al., 2010) .

Young detrital zircons dated as ~290 Ma provide the crucial key to interpret sediment provenance and tectonic setting in eastern South China. Igneous rock of this age occur on Hainan Island (Wuzhishan granite; zircon U-Pb age 262-267 Ma, exposed area 800 km^2; Li et al., 2006) and in the Fujian province (Yangfang alkaline syenite; zircon U-Pb age 254±4 Ma, exposed area 8 km^2; Wang et al., 2005; Daixi-Wufenglou granitoid; zircon U-Pb age 313-318 Ma, exposed area < 5 km^2; Shen et al., 2018; Yu et al., 2013) (Fig. 1). A set of granitoids dated as 292±12.4 Ma (SHRIMP U-Pb dating age) are also known in the Kurosegawa belt of southwest Japan (Sakashima et al. (2003), which mainly consists of Mesozoic-Paleozoic shallow-marine forearc metasediments and igneous or metamorphic basement (Hara et al., 2018). Palaeomagnetic reconstructions suggested that the Kurosegawa belt was located at the eastern edge of the South China block from Late Triassic to Early Cretaceous times (Uno et al., 2011) and thus represents a potential source of ~290 Ma zircon grains found in Longyan sandstones.

5.2 Late Paleozoic magmatism in southeastern South China

Whereas ~290 Ma igneous rocks are rare, ~290 Ma detrital zircons are common in sandstones from SE China to SW Japan. We compiled 1715 detrital zircon ages from

27 previously studied Permian sandstones from SE China (Supplementary Table S4 and quantified the dissimilarities among zircon-age spectra using Kolmogorov-Smirnov statistics visualized by Multidimensional Scaling (MDS, Vermeesch, 2013) (Fig. 6a). The MDS configuration identifies three groups. Group 1 includes samples S1-S3 from the Qinfang basin near Fangcheng Gang city, SW South China (Hu et al., 2014). Group 2 includes samples S4-S18 covering a vast area from Qiongzhou on Hainan island to Nanjing in Jiangsu Province, SE South China (Hu X. et al., 2012; Li X. et al. , 2012; Hu. L. et al., 2017; Li C. et al., 2017). Group 3 includes samples S19-S27 from the Shikoku accretionary complex in the Kurosegawa belt, Japan, (Hara et al., 2018) (Fig. 1).

Fig. 6a shows a clear separation between Groups 1 and 2, indicating different provenances in SW and SE South China, consistently with Hu et al. (2017), and homogeneity of provenance for Group 2 Permian sandstones of SE South China.

In situ Hf isotopic data are available for zircons contained in several Group 2 sandstones (Hu X. et al., 2012; Li X. et al., 2012; Li C. et al., 2017) and indicate a two-stage evolution for 250-350 Ma-aged grains (Fig. 7; Supplementary table S4). A flat trend is indicated by Hf isotopic values of 310-350 Ma zircons, whereas grains younger than ~310 Ma show an overall positive deviation (Fig. 6b). This suggests that the early magmatic phase was associated with melting of ancient crust, whereas new crust started to melt from ~310 Ma onwards.

Age-spectra and Hf isotopes of detrital zircon thus suggest that the Late Carboniferous-Middle Permian igneous event in the source area of Permian sandstones may document the existence of a continental arc along the southeastern boundary of the South China block. This continental arc may have been initiated by the onset of westward subduction of the Paleo-Pacific plate (Li X. et al., 2006, 2012; Hu L. et al., 2015), taking place around 310 Ma when the change in Hf isotopes suggest enhanced melting of new crust.

This continental arc may have prevented detritus from the Cathaysia block to reach the Kurosegawa belt in Japan, as suggested by the lack of ~1850 Ma and early Paleozoic detrital zircons in Group 3 Permian sandstones (Fig. 6b). During the Middle to Late Permian, the Longyan area was probably located in a retro-arc basin, while the forearc basin developed in front of the continental arc hosted the marine sediments found in the Kurosegawa belt and Shikoku area (Fig. 8b).

Based on their geochemical study of S-type granite (317 ± 3 Ma) and monzodiorite/monzogranite (247±2 Ma) exposed in NE Longyan, Shen et al. (2018) proposed that southeasternmost China was located in a back-arc basin related to roll-back of the Paleo-Pacific plate subducting beneath the outboard proto-Japan arc, which was subsequently accreted onto the eastern margin of the South China from the Middle Permian onwards. This scenario, however, does not provide a closure mechanism for the back-arc basin, does not explain the lack of oceanic rocks and sediments, and also fails to explain the high quartz content of Upper Paleozoic clastic rocks in the Longyan area.

5.3 Westward retreat of Lower Permian carbonate platforms in SE China

During the Late Paleozoic, a broad carbonate platform covered most of South China, including the Longyan area, and eventually retreated in the Early Permian (Li, 1997; Mou et al., 1997; Shu et al., 2008a). In order to investigate the cause and spatio-temporal pattern of carbonate-platform retreat, which has not been clarified so far, we have selected four Permian stratigraphic sections from the coastal and interior areas of eastern South China, (Fig. 1 and Fig. 9). In each section, the carbonate platform was replaced by terrigenous siliciclastic rocks with the age of the transition surface mainly constrained by biostratigraphy (Fig.9).

In the Fuding section, located at the southeastern edge of South China, an Upper Carboniferous carbonate unit and the overlying Lower Permian siliciclastic rocks are

preserved in a structural inlier (Hu et al., 2012). These two units are separated by a fault. The depositional age of the carbonates was determined as Bashkirian–Moscovian by fusulinids (*Neostaffella sp., Pseudastaffela, Beedeina sp.,* and *Profusulinella*; Wu and Li, 1990) and conodonts (*Idiognathodus delicate, Neognathodus bassteri, Gondolella sp.,* and *Ozarkodian sp.;* Ying et al., 1994). The depositional age of the siliciclastic unit is constrained as Asselian-Artinskian by the conodonts *Streptognathodus fuchenensis* and *S. elongatus* and by the youngest detrital zircon found at the base of the section (285±3 Ma; Ying et al., 1994; Shen et al., 2019).

In the Longyan section, located to the SW of Fuding and away from the edge of South China, the top of the carbonate unit is constrained as Artinskian-early Kungurian by fusulinids (*Pesudoschwagerian sp., Sphaeroschwagerian sp., Triticites parvulus, Eoparafusulina fusiformis, P. pseudosuni, P. kueichowensis*). The shales at the base of the terrigenous unit contain the ammonites *Waagenoceras sp., Aludoceras cf. altudense*, and *Kufengoceras sp.*, indicating a Roadian-Wordian depositional age (Fujian Institute of Geological Survey, 2015; Shen et al., 2019). The carbonate/siliciclastic transition thus occurred around the Middle/Early Permian boundary.

In the Yanshan section, located farther inland, limestone lenses and calcareous mudrocks of the transition surface contain the brachiopods *Neoplicatifera huangi* and *Dictyoclostus kiangsiensis*, pointing to a Roadian-Wordian age of the carbonate/siliciclastic transition as in the Longyan section (Bureau of Geology and Mineral Resources of Jiangxi Provenance, 1984; Shen et al., 2019).

In the Fengcheng section, located to the west of Yanshan near the northern margin of the Cathaysia block, a disconformity separates marine carbonates containing fusulinids of Wordian-Roadian age (*Neomisellina sp., Neoschwagerina sp.*; Bureau of Geology and Mineral Resources of Jiangxi Province, 1984; Zeng et al., 2010; Shen et

al., 2019) from terrigenous strata containing early Late Permian plant fossils (*Gigantopteris nicotianaefolia, Lobatannularia cf. heianensis, Danaeites rigida, Compsopteris wongii, Cladophlebis permica* and *Pecopteris anderssonii* (Bureau of Geology and Mineral Resources of Jiangxi Province, 1984; Zeng et al., 2010). The carbonate/siliciclastic transition took place here between the Wordian and the Wuchiapingian.

Biostratigraphic evidence thus testifies to a diachronous retreat of the Upper Palaeozoic carbonate platform, progressing from the coast toward the interior of eastern China. The long duration of this process, taking place over ~40 Ma from the Asselian to the Wuchiapingian, indicates a progressive change in paleogeography that we relate to the progressive growth of a continental arc between the Late Carboniferous and the Middle Permian. From 310 to 290 Ma, the continental arc grew in altitude and width in the coastal area (e.g., Fuding), providing detritus to the interior basins thus forcing the progressive retreat of marine carbonates.

6. Conclusions

(1) During the Late Devonian to Early Carboniferous, sandstones in the Longyan area were sourced locally from the Nanling terrane and the western-middle part of the Wuyi terrane. During the Permian, the source area expanded to the southeastern coast of South China.

(2) During the Early Permian, a continental arc grew along the southeastern margin of South China, probably related to the initial westward subduction of the Paleo-Pacific plate. The continental arc was established around 310 Ma, when it started to provide detritus to a vast interior area of southeastern South China.

(3) The diachronous retreat of the Upper Paleozoic carbonate platform from the coastal area to the interior of South China took place during nearly 40 Ma and was

associated with the progressive rise of the continental arc.

Acknowledgments

We thank Bao Liu for his assistance in the field and the laboratory. This study was financially supported by the National Key R&D Plan (Grant No.2017YFC0601405).

References

Bureau of Geology and Mineral Resources of Jiangxi Province, 1984. Regional Geology of Jiangxi Province [in Chinese with English abstract]. Geological Publishing House, Beijing.

Chen, J., Jahn, B., 1998. Crustal evolution of southeastern China: Nd and Sr isotopic evidence. Tectonophysics 284, 101-133.

Cohen, K.M., Finney, S.C., Gibbard, P.L., Fan, J.X., 2013. The ICS international chronostratigraphic chart. Episodes 36, 199-204.

Fujian Institute of Geological Survey, 2015. Regional Geology of Fujian Province. Geological Publishing House, Beijing.

Garzanti, E., 2019. Petrographic classification of sand and sandstone. Earth-science reviews 192, 545-563.

Hara, H., Hirano, M., Kurihara, T., Takahashi, T., Ueda, H., 2018. Permian arc evolution associated with Panthalassa subduction along the eastern margin of the South China block, based on sandstone provenance and U–Pb detrital zircon ages of the Kurosegawa belt, Southwest Japan. Journal of Asian Earth Sciences 151, 112-130.

Hu, L., Cawood, P.A., Du, Y., Xu, Y., Wang, C., Wang, Z., Ma, Q., Xu, X., 2017. Permo-Triassic detrital records of South China and implications for the Indosinian events in East Asia. Palaeogeography, Palaeoclimatology, Palaeoecology 485, 84-100.

Hu, L., Cawood, P.A., Du, Y., Yang, J., Jiao, L., 2015. Late Paleozoic to Early Mesozoic provenance record of Paleo-Pacific subduction beneath South China. Tectonics 34, 986-1008.

Hu, L., Du, Y., Cawood, P.A., Xu, Y., Yu, W., Zhu, Y., Yang, J., 2014. Drivers for late Paleozoic to early Mesozoic orogenesis in South China: Constraints from the sedimentary record. Tectonophysics 618, 107-120.

Hu, X., Huang, Z., Wang, J., Yu, J., Xu, K., Jansa, L., Hu, W., 2012. Geology of the Fuding inlier in southeastern China: Implication for late Paleozoic Cathaysian paleogeography. Gondwana Research 22, 507-518.

Ingersoll, R.V., Bullard, T.F., Ford, R.L., Grimm, J.P., Pickle, J.D., Sares, S.W., 1984. The effect of grain size on detrital modes: a test of the Gazzi-Dickinson point-counting method. Journal of Sedimentary Research 54, 103-116.

Isozaki, Y., Nakahata, H., Zakharov, Y.D., Popov, A.M., Sakata, S., Hirata, T., 2017. Greater South China extended to the Khanka block: Detrital zircon geochronology of middle-upper Paleozoic sandstones in Primorye, Far East Russia. Journal of Asian Earth Sciences 145, 565-575.

Jackson, S.E., Pearson, N.J., Griffin, W.L., Belousova, E.A., 2004. The application of laser ablation-inductively coupled plasma-mass spectrometry to in situ U–Pb zircon geochronology. Chemical Geology 211, 47-69.

Liu, B.J., Xu, X.S., Xia, W.J., Wu, Y.L., Pu, X.C., Chen, H.M., Zhang, J.Q., Pan, X.N., Wang, L.T., et al., 1994. Atlas of the Lithofacies Palaeogeography in Southern China (Sinian-Triassic). Science Press, Peking, pp. 188 (in Chinese).

Li, C., LÜ, X., Hu, X., Yu, J., Sun, G., 2017. Sandstone memory of a Late Paleozoic continental arc in southeast China (Lower Yangtze region) [in Chinese with English abstract]. Chinese Science Bulletin 62, 2951-2966.

Li, X.H., 1997. Timing of the Cathaysia Block formation: Constraints from SHRIMP U-Pb zircon geochronology. Episodes 20, 188-192.

Li, X.H., Li, W.X., Li, Z.X., Lo, C.H., Wang, J., Ye, M.F., Yang, Y.H., 2009. Amalgamation between the Yangtze and Cathaysia Blocks in South China: constraints from SHRIMP U–Pb zircon ages, geochemistry and Nd–Hf isotopes of the Shuangxiwu volcanic rocks. Precambrian Research 174, 117-128.

Li, X.H., Li, Z.X., He, B., Li, W.X., Li, Q.L., Gao, Y.y., Wang, X.C., 2012. The Early Permian active continental margin and crustal growth of the Cathaysia Block: in situ U–Pb, Lu–Hf and O isotope analyses of detrital zircons. Chemical Geology 328, 195-207.

Li, X.H., Li, Z.X., Li, W.X., Wang, Y., 2006. Initiation of the Indosinian Orogeny in South China: evidence for a Permian magmatic arc on Hainan Island. The Journal of geology 114, 341-353.

Li, Z.X., Li, X.H., Wartho, J.A., Clark, C., Li, W.X., Zhang, C.L., Bao, C , 2010. Magmatic and metamorphic events during the early Paleozoic Wuyi- Yunkai orogeny, southeastern South China: New age constraints and pressure-temperature conditions. Geological Society of America Bulletin 122, 772-793.

Li, Z.X, Li, X.H, 2007. Formation of the 1300-km-wide intracontinental orogen and postorogenic magmatic province in Mesozoic South China: A flat-slab subduction model. Geology 35, 179-182.

Li, X. H., Li, Z. X., Li, W. X. 2014. Detrital zircon U–Pb age and Hf isotope constrains on the generation and reworking of Precambrian continental crust in the Cathaysia Block, South China: a synthesis. Gondwana Research, 25(3), 1202-1215.

Ludwig, K., 2011. Isoplot/Ex, Version 4.15: A geochronological toolkit for Microsoft Excel: Geochronology Center Berkeley, v. 4.

Ma, Y.S., Chen, H.D., Wang, G., 2009. Sequence stratigraphy and palaeogeography of South China [in Chinese with English abstract]. Beijing: Science Press.

Mou, C., Qiu, D., Wang, L., 1997. Permian Sedimentary Basins and Sequence Stratigraphy in the Hunan-Hubei-Jiangxi [in Chinese]. Sedimentary Facies and Palaeogeography 17, 1-26.

Müller, R. D., Cannon, J., Qin, X., Watson, R. J., Gurnis, M., Williams, S., et al. 2018. GPlates: Building a virtual Earth through deep time. Geochemistry, Geophysics, Geosystems, 19. doi:10.1029/2018GC007584.

Qie, W., Ma, X., Xu, H., Qiao, L., Liang, K., Guo, W., Song, J., Chen, B., Lu, J., 2019. Devonian integrative stratigraphy and timescale of China. Science China Earth Sciences 62, 112-134.

Sakashima, T., Terada, K., Takeshita, T., Sano, Y., 2003. Large-scale displacement along the Median Tectonic Line, Japan: evidence from SHRIMP zircon U–Pb dating of granites and gneisses from the South Kitakami and paleo-Ryoke belts. Journal of Asian Earth Sciences 21, 1019-1039.

Scotese, C.R., 2016. PALEOMAP PaleoAtlas for GPlates and the PaleoData Plotter Program, PALEOMAP Project. http://www.earthbyte.org/paleomap-paleoatlas-for-gplates.

Shen, L., Yu, J., O'Reilly, S., Griffin, W., 2018. Tectonic Switching of Southeast China in the Late Paleozoic. Journal of Geophysical Research: Solid Earth 123(10), 8508-8526.

Shen, S., Zhang, H., Zhang, Y., Yuan, D., Chen, B., He, W., Mu, L., Lin, W., Wang, W., Chen, J., 2019. Permian integrative stratigraphy and timescale of China. Science China Earth Sciences 62, 154-188.

Shu, L.S., 2006. Pre-Devonian tectonic evolution of South China: from Cathaysian block to Caledonian folded orogenic belt. Geological Journal of China Universities 12, 418–431.

Shu, L., Faure, M., Wang, B., Zhou, X., Song, B., 2008a. Late Palaeozoic–Early Mesozoic geological features of South China: Response to the Indosinian collision events in Southeast Asia. Comptes Rendus Geoscience 340, 151-165.

Shu, L.S., Ping, D., Yu, J.H., Wang, Y.B., Jiang, S.Y., 2008b. The age and tectonic environment of the rhyolitic rocks on the western side of Wuyi Mountain, South China. Science China Earth Sciences 51, 1053-1063.

Uno, K., Furukawa, K., Hada, S., 2011. Margin-parallel translation in the western Pacific: Paleomagnetic evidence from an allochthonous terrane in Japan. Earth and Planetary Science Letters 303, 153-161.

Vermeesch, P., 2004. How many grains are needed for a provenance study?. Earth and Planetary Science Letters, 224(3-4), 441-451.

Vermeesch, P., 2012. On the visualisation of detrital age distributions. Chemical Geology 312, 190-194.

Vermeesch, P., 2013. Multi-sample comparison of detrital age distributions. Chemical Geology 341, 140-146.

Vermeesch, P., Resentini, A., Garzanti, E., 2016. An R package for statistical provenance analysis. Sedimentary Geology 336, 14-25.

Wan, Y., Liu, D., Xu, M., Zhuang, J., Song, B., Shi, Y., Du, L., 2007. SHRIMP U–Pb zircon geochronology and geochemistry of metavolcanic and metasedimentary rocks in Northwestern Fujian, Cathaysia block, China: Tectonic implications and the need to redefine lithostratigraphic units. Gondwana Research 12, 166-183.

Wang, Q., Li, J.W., Jian, P., Zhao, Z.H., Xiong, X.L., Bao, Z.W., Xu, J.F., Li, C.F., Ma, J.L., 2005. Alkaline syenites in eastern Cathaysia (South China): link to Permian–Triassic transtension. Earth & Planetary Science Letters 230, 339-354.

Wang, X., Hu, K., Qie, W., Sheng, Q., Chen, B., Lin, W., Yao, L., Wang, Q., Qi, Y., Chen, J., 2019. Carboniferous integrative stratigraphy and timescale of China. Science China Earth Sciences 62, 135-153.

Wang, X.L., Zhou, J.C., Griffin, W.a., Wang, R.C., Qiu, J.S., O'Reilly, S., Xu, X., Liu, X.-M., Zhang, G.-L., 2007. Detrital zircon geochronology of Precambrian basement sequences in the Jiangnan orogen: dating the assembly of the Yangtze and Cathaysia Blocks. Precambrian Research 159, 117-131.

Wang, Y., Zhang, F., Fan, W., Zhang, G., Chen, S., Cawood, P.A., Zhang, A., 2010. Tectonic setting of the South China Block in the early Paleozoic: Resolving intracontinental and ocean closure models from detrital zircon U- Pb geochronology. Tectonics 29, 10.1029/2010TC002750.

Wu, F.-Y., Yang, Y.-H., Xie, L.-W., Yang, J.-H., Xu, P., 2006. Hf isotopic compositions of the standard zircons and baddeleyites used in U–Pb geochronology. Chemical Geology 234, 105-126.

Wu, Q., Li, X., 1990. Carboniferous stratigraphy and tectonic environment in Fuding, Fujian [in Chinese]. Reg. Geol. China 4, 327-333.

Wu Y.B., Zheng Y.F., 2004. Genesis of zircon and its constraints on interpretation of U-Pb age. Chinese Science Bulletin, 49(15), 1554-1569.

Xia, Y., Xu, X.S., Zhu, K.Y., 2012. Paleoproterozoic S- and A-type granites in southwestern Zhejiang: Magmatism, metamorphism and implications for the crustal evolution of the Cathaysia basement. Precambrian Research s 216–219, 177-207.

Xu, X., O'Reilly, S.Y., Griffin, W.L., Wang, X., Pearson, N.J., He, Z., 2007. The crust of Cathaysia: Age, assembly and reworking of two terranes. Precambrian Research 158, 51-78.

Yao, W.H., Li, Z.X., Li, W.X., Li, X.H., Yang, J.H., 2014. From Rodinia to Gondwanaland: A tale of detrital zircon provenance analyses from the southern Nanhua Basin, South China. American Journal of Science 314,

278-313.

Ying, Z.E., Ding, B.L., Bi, Z.Q., 1994. Discovery of Mid-Late Carboniferous conodonts in the Nanxi "Tectonic window" in Fuding County, Fujian.[in Chinese]. Volcanology and Mineral Resources 15, 43-48.

Yu, J.-H., Liu, Q., Hu, X., Wang, Q., O'Reilly, S.Y., 2013. Late Paleozoic magmatism in South China: Oceanic subduction or intracontinental orogeny? Chinese Science Bulletin 58, 788-795.

Yu, J.-H., O'Reilly, S.Y., Wang, L., Griffin, W.L., Zhou, M.-F., Zhang, M., Shu, L., 2010. Components and episodic growth of Precambrian crust in the Cathaysia Block, South China: evidence from U–Pb ages and Hf isotopes of zircons in Neoproterozoic sediments. Precambrian Research 181, 97-114.

Yu, J.-H., Wang, L., O'reilly, S., Griffin, W., Zhang, M., Li, C., Shu, L., 2009. A Paleoproterozoic orogeny recorded in a long-lived cratonic remnant (Wuyishan terrane), eastern Cathaysia Block, China. Precambrian Research 174, 347-363.

Zeng, S., You, W., Qin, Z., 2010. The later period of Early Permian-Later Permian strata in the central-western Jiangxi Province, China. [in Chinese with English Abstract]. Geological Bulletin of China 29, 1619-1632.

Zhang, X., Takeuchi, M., Lee, H.Y., 2019. Tracing the origin of Southwest Japan using the Hf isotopic composition of detrital zircons from the Akiyoshi Belt. Terra Nova 31, 11-17.

Zhao, G., Cawood, P. A. 2012. Precambrian geology of China. Precambrian Research, 222, 13-54.

Zhou, X., Li, W., 2000. Origin of Late Mesozoic igneous rocks in Southeastern China: Implications for lithosphere subduction and underplating of mafic magmas. Tectonophysics 326, 269-287.

Figure and table captions

Figure 1. Tectonic framework of eastern China and southwestern Japan. Simplified from Yu et al. (2010) and Uno et al. (2011). See text for references of igneous and detrital zircon data.

Figure 2. Stratigraphic framework for the Longyan area, indicating sample positions and depositional environments.

Figure 3. Detrital modes of Paleozoic sandstones in the Longyan and surrounding areas of SE South China. **A**) QFL plot (Q, quartz; F, feldspar; L, lithic fragments); **B**) LvLmLs plot (Lv, volcanic; Lm, metamorphic; Ls,sedimentary). Sandstone classification in QFL plot after Garzanti (2019). Previous datasets from the Yong'an, Fuding, and Nanjing areas from Hu et al. (2015), Hu et al. (2012) and Li et al. (2017), respectively.

Figure 4. U-Pb age spectra of detrital zircon in Upper Paleozoic sandstones exposed in the Longyan area. Arrows indicate the depositional ages constrained by fossils reported in Fujian Institute of Geological Survey (2015).

Figure 5. Plot of detrital zircon U-Pb age *vs. in situ* εHf (t) for upper Paleozoic sandstones exposed in the Longyan area. **A**, **B**) Middle-Upper Permian sandstones; **C**, **D**) Upper Devonian-Lower Carboniferous sandstones. B and D are enlarged displays of the 200-500Ma interval in A and C.

Figure 6. MDS and KDE plots based on age spectra of detrital zircons. **A**) MDS map

of Kolmogorov–Smirnov dissimilarities drawn using the software package *provenance* (Vermeesch et al., 2016). Solid and dashed lines link nearest and second-nearest neighbor in K-S space, respectively. Samples: S1-S3 from Hu et al. (2014), S4-S18 from this study, Hu X. et al. (2012), Li X. et al. (2012), Hu. L. et al. (2017), and Li C. et al. (2017); S19-S27 from Hara et al. (2018). **B**) Differences among spectra of samples belonging to Groups 1, 2, and 3.

Figure 7. Age *vs.* εHf (t) plot of young detrital zircons (250-350 Ma) contained in Permian sandstones of SE South China. Data for Middle and Upper Permian samples from this study, Li X. et al. (2012), and Li C. et al. (2017); data for Lower Permian samples from Hu X. et al. (2012).

Figure 8. Paleogeography of South China. A) Late Devonian to Early Carboniferous; **B**) Middle Permian. Yellow areas indicate igneous rocks considered as products of the continental arc (locations inferred from their current position in South China and referred to the paleogeographic maps in the PALEOMAP Atlas, Scotese, 2016). From north to south: Permian Wuzhishan granite on Hainan island (Li et al., 2006); Permian Yangfang alkaline syenites in the Fujian province (Wang et al., 2005)Lower Triassic Houzhang complex comprising monzodiorite and monzogranite (Shen et al., 2018). Time slices generated by *Gplates* software (Müller, et al., 2018).

Figure 9. Diachronous retreat of the Upper Carboniferous-Lower Permian carbonate platform in SE South China (chronostratigraphy after Cohen et al., 2013; Qie et al., 2019; Shen et al., 2019; Wang et al., 2019; lithological columns after Bureau of Geology and Mineral Resources of Jiangxi Province, 1984; Hu X. et al., 2012; Fujian Institute of Geological Survey, 2015).

Table 1 Point counting results of Upper Devonian-Upper Permian sandstones in Longyan area, South China

Formation	Sample	Q	F	Lv	Lm	Ls	Sum QFL
Luokeng (P3l)	08MTK07	296	102	1	1	8	408
Cuipingshan (P3cp)	08MTK05	348	51	29	3	6	437
Cuipingshan (P3cp)	08MTK01	308	63	21	2	9	403
Cuipingshan (P3cp)	08MTK02	344	42	10	1	5	402
Tongziyan (P2t)	10SW03	356	37	8	0	4	405
Tongziyan (P2t)	08MTK03	377	28	22	2	5	434
Tongziyan (P2t)	08MTK04	365	22	19	2	2	410
Lindi (C1l)	08TZK09	363	32	12	3	3	413
Lindi (C1l)	10LB06	297	60	36	13	1	407
Lindi (C1l)	10TZK25	332	46	19	2	2	401
Lindi (C1l)	10TZK24	345	32	18	5	0	400
Taozikeng (D3tz)	10TZK11	322	69	10	27	0	428

Taozikeng (D3tz)	10TZK10	309	52	16	26	4	407
Taozikeng (D3tz)	08TZK06	341	40	12	13	0	406
Tianwadong (D3t)	10TZK03	382	23	4	24	0	433
Tianwadong (D3t)	10TZK02	366	12	10	19	1	408
Tianwadong (D3t)	08TZK05	325	37	10	31	0	403
Tianwadong (D3t)	08TZK04	371	23	4	22	2	422

Note: Q-quartz; F-feldspar; L-lithic fragment (Lv-volcanic; Lm-metamorphic; Ls-sedimentary)

Credit Author Statement

Li Chao: Conceptualization; Formal analysis; Investigation; Writing - Original Draft
Hu xiumian: Conceptualization; Funding acquisition Writing - Review & Editing; Supervision
Wang Jiangang: Resources; Project administration
Pieter Vermeesch: Writing - Review & Editing
Eduardo Garzanti: Writing - Review & Editing

Highlights

- A continental arc once occurred during ~310-250 Ma along the southeast margin of the South China block.
- Following the occurrence of the continental arc, a retreat of a broad carbonate platform towards inland South China took place during the Early and Late Permian.

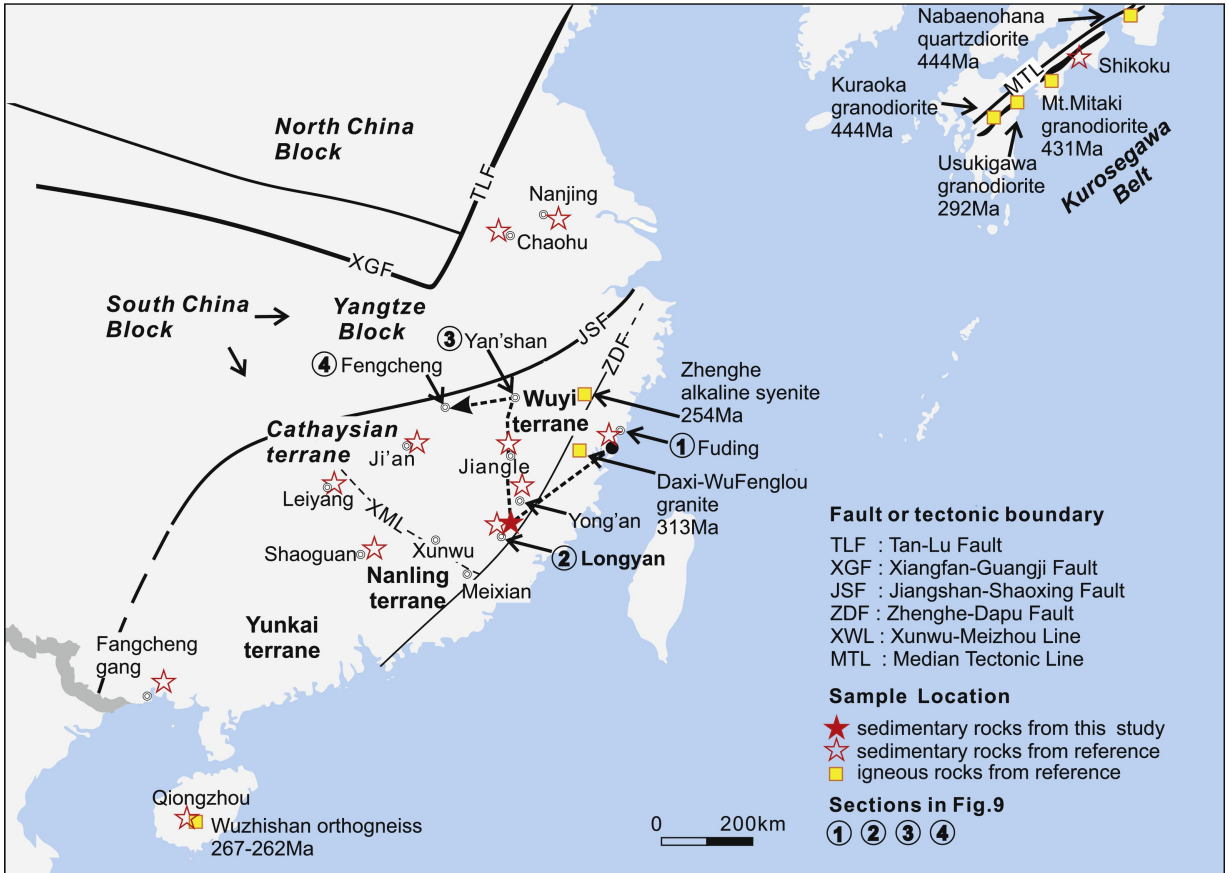
North China Block
South China Block
Yangtze Block
TLF
XGF
JSF
ZDF
XWL
MTL
Nanjing
Chaohu
③ Yan'shan
④ Fengcheng
Wuyi terrane
Zhenghe alkaline syenite 254Ma
① Fuding
Daxi-WuFenglou granite 313Ma
Cathaysian terrane
Ji'an
Jiangle
Leiyang
Yong'an
② Longyan
Shaoguan
Xunwu
Nanling terrane
Meixian
Yunkai terrane
Fangcheng gang
Qiongzhou
Wuzhishan orthogneiss 267-262Ma
Nabaenohana quartzdiorite 444Ma
Shikoku
Kuraoka granodiorite 444Ma
Mt.Mitaki granodiorite 431Ma
Usukigawa granodiorite 292Ma
Kurosegawa Belt
0 200km
Fault or tectonic boundary
TLF : Tan-Lu Fault
XGF : Xiangfan-Guangji Fault
JSF : Jiangshan-Shaoxing Fault
ZDF : Zhenghe-Dapu Fault
XWL : Xunwu-Meizhou Line
MTL : Median Tectonic Line
Sample Location
sedimentary rocks from this study
sedimentary rocks from reference
igneous rocks from reference
Sections in Fig.9
① ② ③ ④

Figure 1

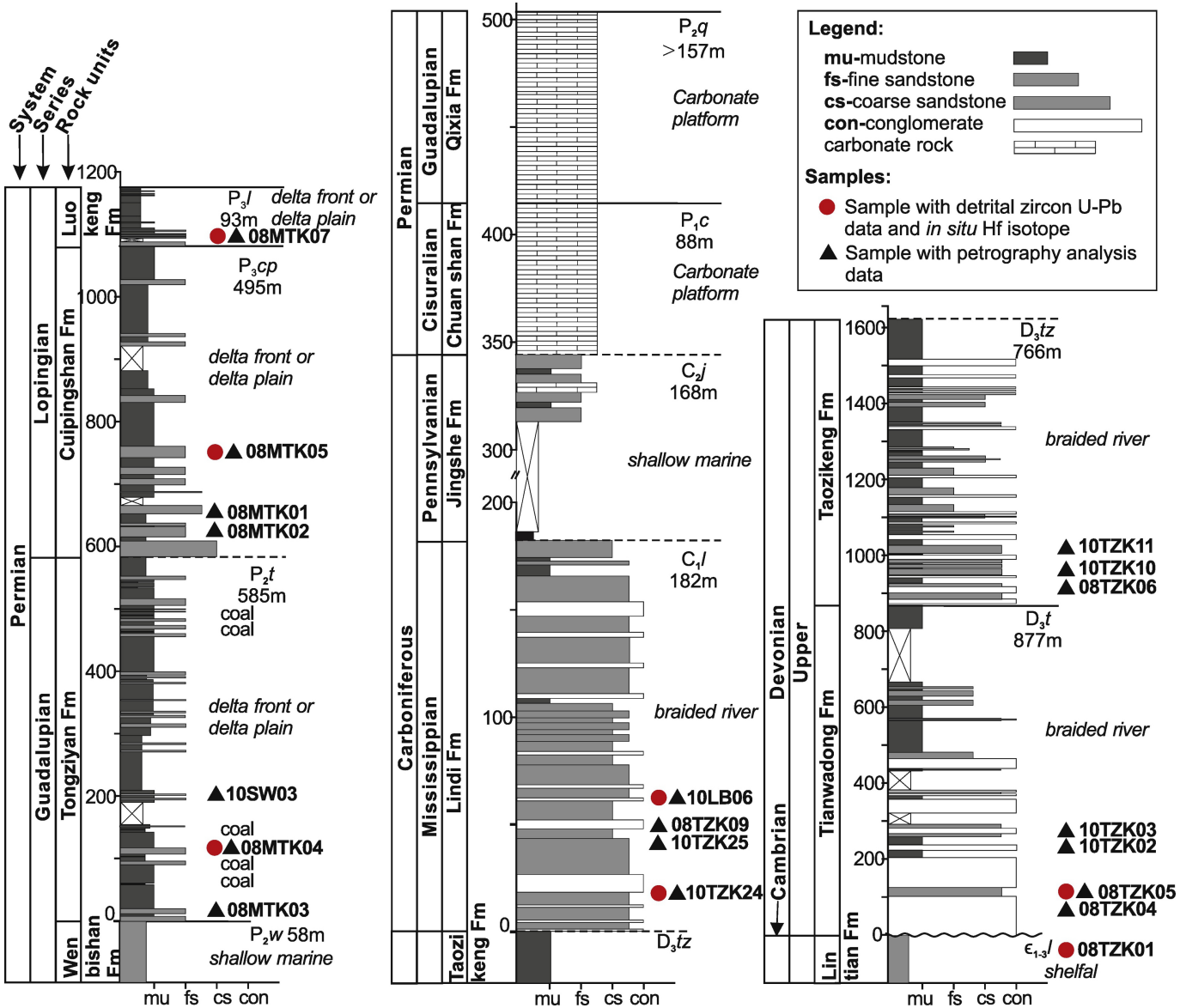
System
Series
Rock units
Permian
Lopingian
Guadalupian
Luo keng Fm
Cuipingshan Fm
Tongziyan Fm
Wen bishan Fm
1200
1000
800
600
400
200
0
P3l 93m delta front or delta plain
08MTK07
P3cp 495m
delta front or delta plain
08MTK05
08MTK01
08MTK02
P2t 585m
coal
coal
delta front or delta plain
10SW03
coal
08MTK04
coal
coal
08MTK03
P2w 58m
shallow marine
mu fs cs con
Permian
Guadalupian
Qixia Fm
Cisuralian
Chuan shan Fm
Carboniferous
Pennsylvanian
Jingshe Fm
Mississippian
Lindi Fm
Taozi keng Fm
500
400
350
300
200
100
0
P2q >157m
Carbonate platform
P1c 88m
Carbonate platform
C2j 168m
shallow marine
C1l 182m
braided river
10LB06
08TZK09
10TZK25
10TZK24
D3tz
mu fs cs con
Legend:
mu-mudstone
fs-fine sandstone
cs-coarse sandstone
con-conglomerate
carbonate rock
Samples:
Sample with detrital zircon U-Pb data and in situ Hf isotope
Sample with petrography analysis data
Devonian
Upper
Cambrian
Taozikeng Fm
Tianwadong Fm
Lin tian Fm
1600
1400
1200
1000
800
600
400
200
0
D3tz 766m
braided river
10TZK11
10TZK10
08TZK06
D3t 877m
braided river
10TZK03
10TZK02
08TZK05
08TZK04
ϵ1-3l
08TZK01
shelfal
mu fs cs con

Figure 2

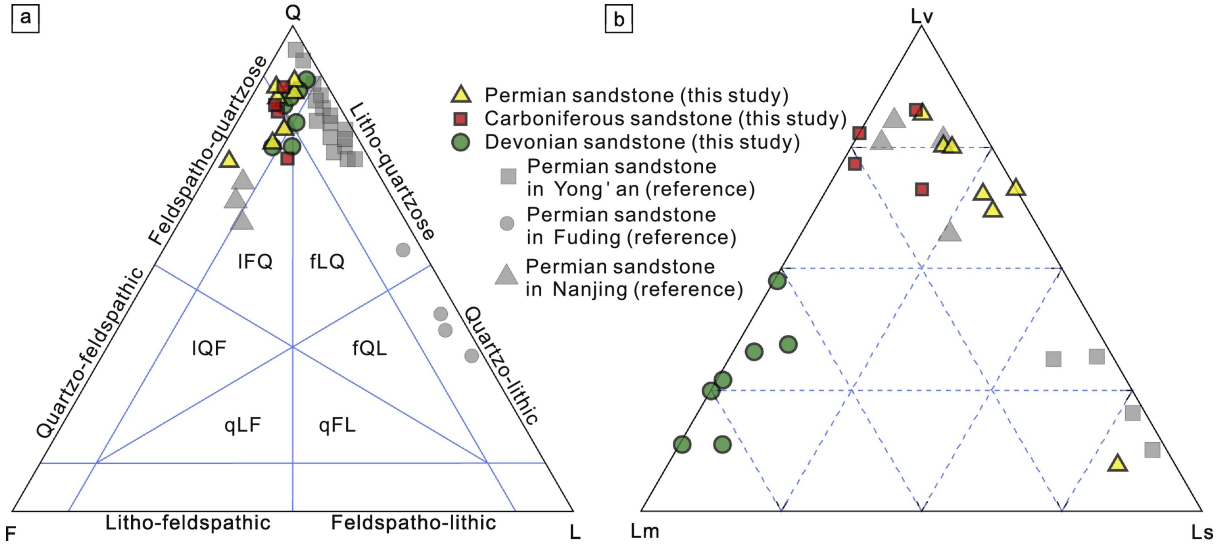
a
Q
F
L
Feldspatho-quartzose
Litho-quartzose
Quartzo-feldspathic
Quartzo-lithic
Litho-feldspathic
Feldspatho-lithic
lFQ
fLQ
lQF
fQL
qLF
qFL
Permian sandstone (this study)
Carboniferous sandstone (this study)
Devonian sandstone (this study)
Permian sandstone in Yong' an (reference)
Permian sandstone in Fuding (reference)
Permian sandstone in Nanjing (reference)
b
Lv
Lm
Ls

Figure 3

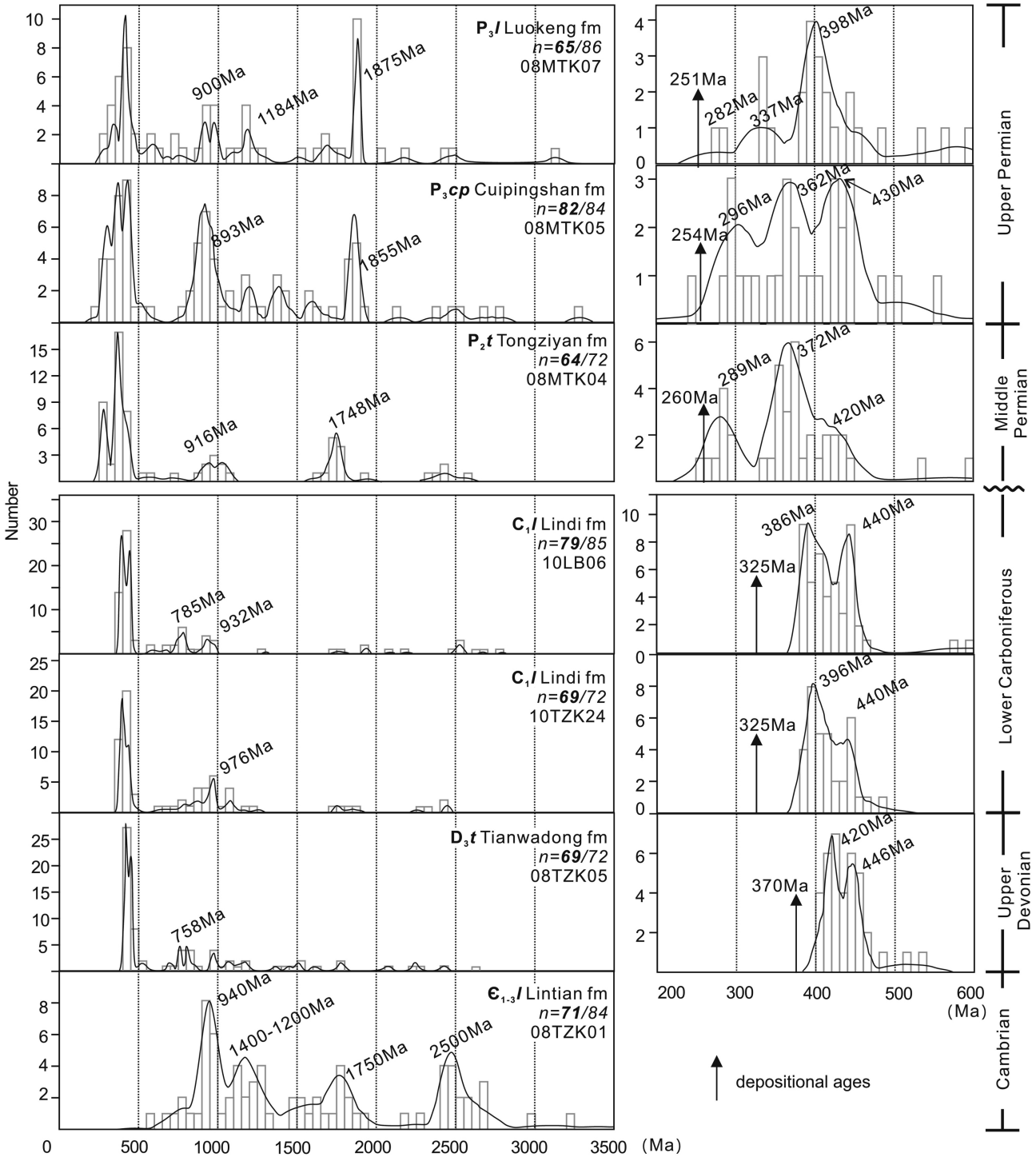
P3l Luokeng fm
n=65/86
08MTK07
900Ma
1184Ma
1875Ma
P3cp Cuipingshan fm
n=82/84
08MTK05
893Ma
1855Ma
P2t Tongziyan fm
n=64/72
08MTK04
916Ma
1748Ma
C1l Lindi fm
n=79/85
10LB06
785Ma
932Ma
C1l Lindi fm
n=69/72
10TZK24
976Ma
D3t Tianwadong fm
n=69/72
08TZK05
758Ma
Cϵ1-3l Lintian fm
n=71/84
08TZK01
940Ma
1400-1200Ma
1750Ma
2500Ma
251Ma
282Ma
337Ma
398Ma
254Ma
296Ma
362Ma
430Ma
260Ma
289Ma
372Ma
420Ma
325Ma
386Ma
440Ma
325Ma
396Ma
440Ma
370Ma
420Ma
446Ma
depositional ages
Number
(Ma)
Upper Permian
Middle Permian
Lower Carboniferous
Upper Devonian
Cambrian

Figure 4

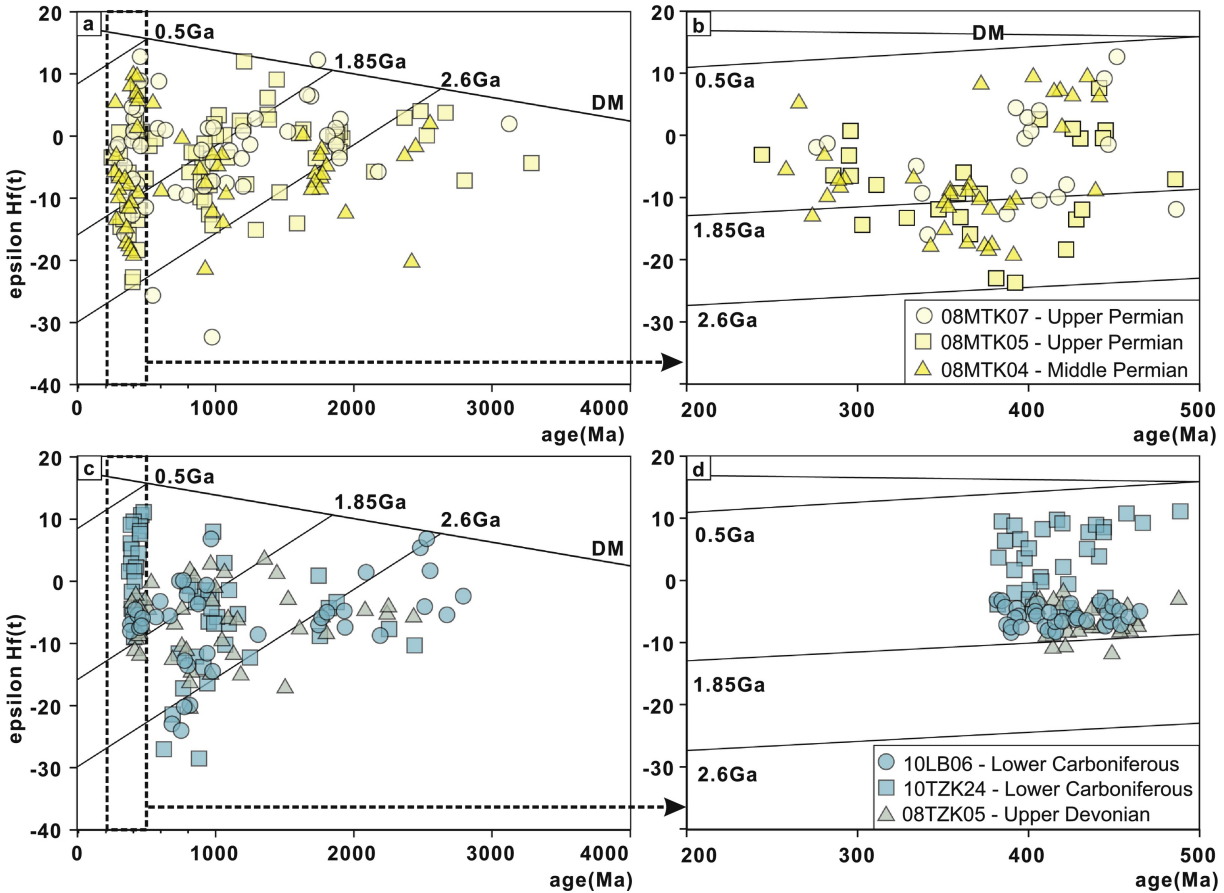
a
0.5Ga
1.85Ga
2.6Ga
DM
epsilon Hf(t)
age(Ma)
b
DM
0.5Ga
1.85Ga
2.6Ga
08MTK07 - Upper Permian
08MTK05 - Upper Permian
08MTK04 - Middle Permian
age(Ma)
c
0.5Ga
1.85Ga
2.6Ga
DM
epsilon Hf(t)
age(Ma)
d
0.5Ga
1.85Ga
2.6Ga
10LB06 - Lower Carboniferous
10TZK24 - Lower Carboniferous
08TZK05 - Upper Devonian
age(Ma)

Figure 5

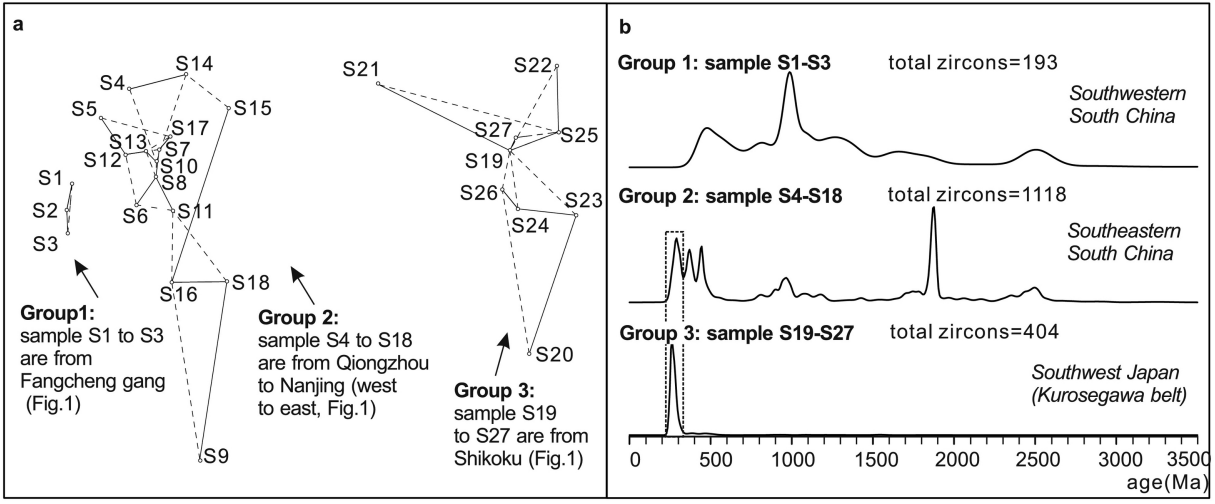
a
S14
S4
S15
S5
S17
S13
S7
S12
S10
S8
S1
S2
S6
S11
S3
S18
S16
S9
Group1:
sample S1 to S3
are from
Fangcheng gang
(Fig.1)
Group 2:
sample S4 to S18
are from Qiongzhou
to Nanjing (west
to east, Fig.1)
S21
S22
S27
S25
S19
S26
S23
S24
S20
Group 3:
sample S19
to S27 are from
Shikoku (Fig.1)
b
Group 1: sample S1-S3
total zircons=193
Southwestern
South China
Group 2: sample S4-S18
total zircons=1118
Southeastern
South China
Group 3: sample S19-S27
total zircons=404
Southwest Japan
(Kurosegawa belt)
0
500
1000
1500
2000
2500
3000
3500
age(Ma)

Figure 6

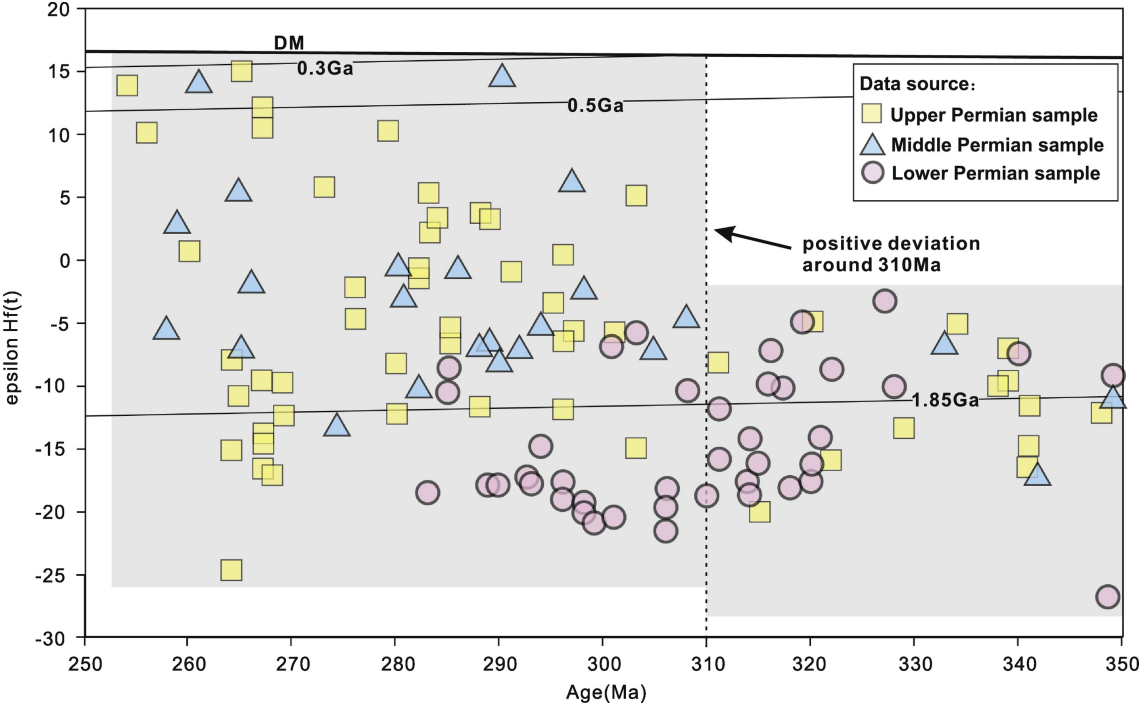
DM
0.3Ga
0.5Ga
1.85Ga
Data source:
Upper Permian sample
Middle Permian sample
Lower Permian sample
positive deviation
around 310Ma
epsilon Hf(t)
Age(Ma)
20
15
10
5
0
-5
-10
-15
-20
-25
-30
250
260
270
280
290
300
310
320
330
340
350

Figure 7

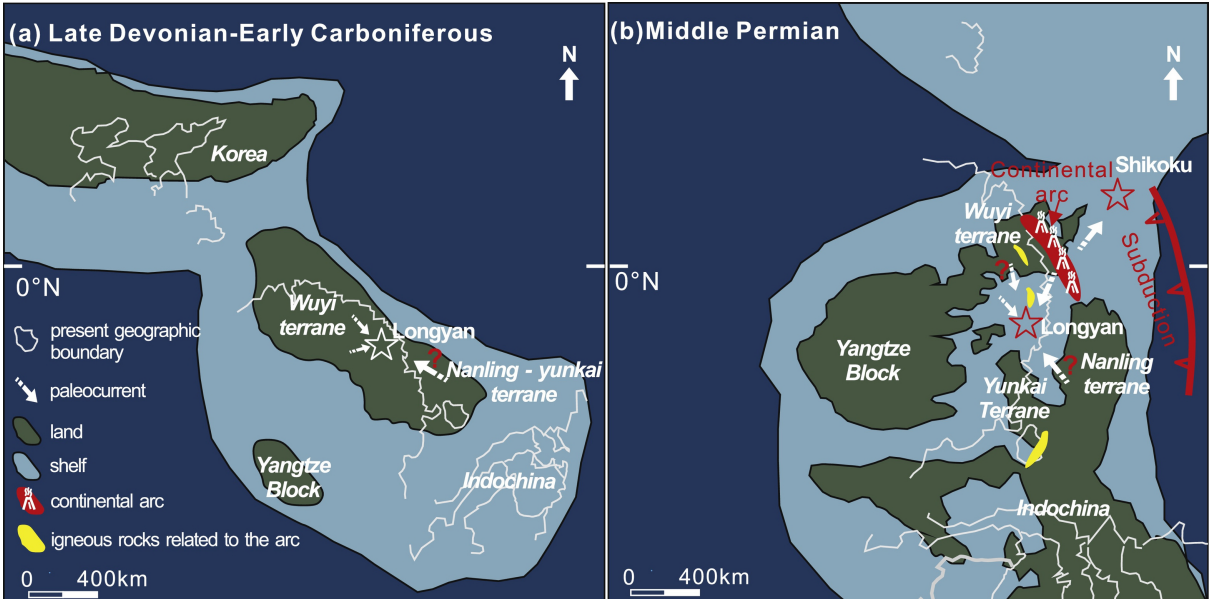
(a) Late Devonian-Early Carboniferous
N
Korea
0°N
present geographic boundary
paleocurrent
land
shelf
continental arc
igneous rocks related to the arc
0 400km
Wuyi terrane
Longyan
Nanling - yunkai terrane
Yangtze Block
Indochina
(b)Middle Permian
N
Continental arc
Shikoku
Subduction
Wuyi terrane
0°N
Yangtze Block
Longyan
Nanling terrane
Yunkai Terrane
Indochina
0 400km

Figure 8

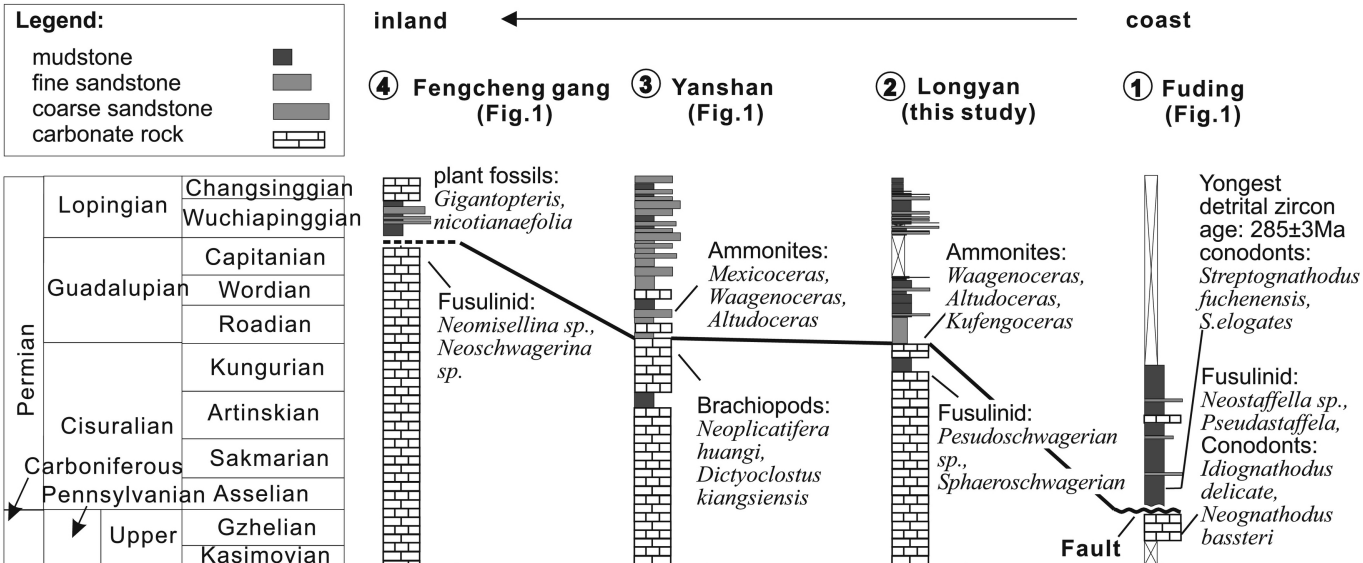
Legend:
mudstone
fine sandstone
coarse sandstone
carbonate rock
inland
coast
④ Fengcheng gang (Fig.1)
③ Yanshan (Fig.1)
② Longyan (this study)
① Fuding (Fig.1)
Permian
Lopingian
Changsinggian
Wuchiapinggian
Guadalupian
Capitanian
Wordian
Roadian
Cisuralian
Kungurian
Artinskian
Sakmarian
Carboniferous
Pennsylvanian
Asselian
Upper
Gzhelian
Kasimovian
plant fossils:
Gigantopteris, nicotianaefolia
Fusulinid:
Neomisellina sp., Neoschwagerina sp.
Ammonites:
Mexicoceras, Waagenoceras, Altudoceras
Brachiopods:
Neoplicatifera huangi, Dictyoclostus kiangsiensis
Ammonites:
Waagenoceras, Altudoceras, Kufengoceras
Fusulinid:
Pesudoschwagerian sp., Sphaeroschwagerian
Yongest detrital zircon age: 285±3Ma
conodonts:
Streptognathodus fuchenensis, S.elogates
Fusulinid:
Neostaffella sp., Pseudastaffela,
Conodonts:
Idiognathodus delicate, Neognathodus bassteri
Fault

Figure 9